Simulation of the Precipitation of Silver Bromide Photographic Emulsions

Nucleation and crystal growth processes involved in the batch precipitation of photographic emulsions by the addition of silver nitrate to an aqueous solution of bromide and gelatin have been reasonably successfully modeled. Simulation predicts the known increase in average crystal size with increased addition time, with increased temperature, and with increased halide levels. Solubility is related to crystal size by the Gibbs-Thomson equation. The predicted decrease in the number of crystals during the course of precipitation is similar to published data, but there are quantitative differences. The model is very sensitive to variations in the constant in the growth equation, but not to variations in the constants in the nucleation equation.

GEOFFREY MARGOLIS
and
EDGAR B. GUTOFF

Emulsion Development Laboratory
Polaroid Corporation
Waltham, Massachusetts 02154

SCOPE

Photographic emulsions are normally made by the slow addition of an aqueous silver nitrate solution to an agitated, aqueous halide-gelatin solution in a batch reactor. In order to test our understanding of the precipitation mechanisms we developed a mathematical model that describes nucleation and crystal growth. A satisfactory model should predict the course of precipitation as we know it, should predict the effects of changing variables, and should help in determining the degree of control needed in the process.

Previous work has indicated that the precipitation can be considered as occurring in three stages. In the first, very short stage, no precipitation occurs—only the silver supersaturation increases. In the second stage, lasting under a minute, both nucleation and crystal growth take place. Nucleation of very fine crystals occurs in the vicinity of the silver nitrate jet, and these embryos apparently coalesce to form effective nuclei of about 0.1 μm in size. Thus nucleation can be considered as forming these effective nuclei. In the third stage which lasts until all the silver nitrate is added—normally up to an hour—the solution is undersaturated with respect to the effective nuclei. Here nucleation is considered as no longer occurring. However, because of the decrease in solubility with increase in size, the solution is still supersaturated with respect to the larger crystals and they continue to grow. At the same time physical ripening occurs; that is, the smaller particles dissolve and contribute to the growth of the larger particles. Thus there is a decrease in the total number of crystals present.

The material balance equation for silver equates the rate of accumulation of silver in solution to the rate of addition of silver nitrate minus the rate of removal of silver by nucleation and by growth. The growth rate is taken to be proportional to the supersaturation. The Gibbs-Thomson equation is used to relate the solubility to the crystal size. Because the solubility varies with size, the supersaturation and therefore the growth rate also vary with size. Thus the partial differential equation expressing the population balance cannot be integrated to ordinary differential equations in terms of moments of the distribution as is customarily done.

Instead of using the population balance equation, finite difference techniques were used. During the nucleation phase a new class of crystals is considered as being formed in each time interval and all crystal classes are accounted for separately throughout the precipitation period.

CONCLUSIONS AND SIGNIFICANCE

This mathematical model of the batch precipitation of silver bromide photographic emulsions by the slow addition of silver nitrate to an aqueous halide-gelatin solution predicts the known effects of longer addition times, higher temperatures, and higher bromide concentrations on increasing the mean crystal size; tends to confirm the reported observation that the growth kinetics rather than mass transfer is the rate controlling step in the growth of the crystals; and indicates that crystal growth rather than nucleation is the controlling factor in the overall process. In addition, it shows the short period during which effective nucleation occurs and also shows the decrease in the number of crystals that occurs during precipitation due to physical ripening.

The model needs further improvement in that it predicts a crystal size distribution skewed to the left whereas photographic emulsions of this type are skewed to the right. Improving the model by taking into account the formation of twinned crystals, which is known to occur, does not correct the skewness. Perhaps the growth rate should be taken as proportional to a power of the supersaturation.

In addition, the model predicts a crystal size distribution that is narrower than found in experimental emulsions. On taking into account the formation of twinned crystals the crystal size distribution becomes too broad.

The model does, however, point out the importance of the short initial period during which nucleation occurs. Control during this short period is obviously difficult in a batch process.

Correspondence concerning this paper should be addressed to E. B. Gutoff. Dr. Margolis started this work while at MIT and a consultant to Polaroid. He is with Westreco, Inc., Marysville, Ohio 43040.

Photographic emulsions consist of dispersions of silver halide crystals, about 1 μm in size, in a protective colloid such as gelatin. Most commercial photographic emulsions are made by adding silver nitrate to a vessel containing an aqueous solution of excess halide and of gelatin. When the silver nitrate is added slowly, this method is called the single jet technique (Duffin, 1966) and this is the system we will study. After precipitation of the silver halide, the dispersion is often held at temperature to allow physical or Ostwald ripening to take place. During this stage fine crystals dissolve due to their higher solubility while the coarser crystals grow. Ammonia is sometimes added to increase the growth rates and to modify the crystal habit.

The sensitometric properties of the finished photographic emulsion are to a large extent dependent on the crystal size distribution, and it is therefore important to control this distribution. This work aims to use the nucleation and growth equations of the silver halides to predict the particle size distribution of the photographic emulsion in order to better understand how to control it. Emulsions of high light sensitivity are based on silver bromide with small percentages of silver iodide; this study will consider a simpler system based on pure silver bromide.

It is known that physical ripening takes place during the precipitation of the silver halide (Gutoff et al., 1974); that is, the concentration of dissolved silver halide is such that the solution is supersaturated with respect to the larger crystals and therefore they grow, while at the same time it is undersaturated with respect to smaller crystals and so they dissolve. The number of crystals decreases with time, from times under 1 min. for precipitations of up to 60 min. The model must first show this decrease in the number of crystals during the precipitation.

The precipitation vessel can be regarded as containing two regions (Gutoff et al., 1974): the well-mixed bulk of the vessel and also a region of negligible volume in the vicinity of the silver nitrate jet. In the region of the jet nucleation takes place. Fast flocculation or coalescence also appears to take place in this region to give effective nuclei of perhaps 0.1 μm diameter. These nuclei are fed into the bulk. When the supersaturation is high enough at the start of the precipitation, these nuclei grow. Later on, when the concentration of dissolved silver halide is lowered to the point where the solution is no longer saturated with respect to these nuclei, they dissolve and act just as a source of additional silver halide for the crystals that are growing.

This picture can be further simplified and the precipitation can be divided into three stages. In the first stage no precipitation occurs—the added silver nitrate just builds up the supersaturation to the point where nucleation occurs. In the second stage, nucleation occurs at the size of the effective nuclei, ~0.1 μm, and the existing crystals grow. In the third stage the solution is undersaturated with respect to the nuclei and so nucleation is considered as no longer occurring; only growth and physical ripening occur. We will now express these concepts mathematically.

Because the solubility and therefore the growth rates vary with particle size, the partial differential equation for the population balance that is customarily written (Randolph and Larson, 1971) cannot be integrated to ordinary differential equations in terms of moments of the distribution. Instead during each time interval in the nucleation stage a new class of crystals is formed, and all classes are accounted for throughout the precipitation period.

MATERIAL BALANCE, BASED ON SILVER

The rate of accumulation of dissolved silver is equal to the rate of addition of silver nitrate minus the rate of removal of silver by nucleation and by growth. Thus, assuming spherical crystals,

$$\frac{d(CV)}{dt} = V\frac{dC}{dt} + CF = FC^0_{Ag} - NV\frac{4}{3}\pi r_0^3\rho - \int_0^\infty G_r 4\pi r^2 f dr \cdot V\rho \quad (1)$$

The first term on the right-hand side of Equation (1) represents the addition rate of silver to the system. The second term represents the rate of removal of silver by the formation of nuclei of radius r_0 μm. The third term represents the rate of removal of silver by growth on existing crystals. The surface area of a crystal is $4\pi r^2$, and fdr is the number of crystals per liter of size between r and $r + dr$. The terms representing nucleation and growth are omitted when they do not apply.

All the concentration dependent terms, namely C, N, and G_r, will now be expressed in terms of G_∞, the radial growth rate for infinitely large particles. McCabe's rule will be assumed to hold so that the growth rate will be taken only as a function of supersaturation. However, as the solubility varies with crystal size, the supersaturation and therefore the growth rate will also be a function of size. Assuming that the exponent in the growth equation is unity, then, for large crystals

$$G_\infty = k_1(C - C_\infty) \quad (2)$$

and the rate of change of the concentration of dissolved silver is

$$\frac{dC}{dt} = \frac{1}{k_1}\frac{dG_\infty}{dt} + \frac{dC_\infty}{dC_{Br}}\cdot\frac{dC_{Br}}{dt} \quad (3)$$

In the presence of excess bromide, dissolved silver forms complex species of the type $AgBr_n^{-(n-1)}$. Based on a recent study, the total solubility of all these species at 18°C is (Sillén, 1964)

$$C_\infty^{18°} = (2.09 \times 10^{-13}/C_{Br}) + 1.02 \times 10^{-8} + 9.33 \times 10^{-6}C_{Br} + 1.05 \times 10^{-4}C^2_{Br} + 1.26 \times 10^{-4}C^3_{Br} + 2.09 \times 10^{-5}C^4_{Br} \quad (4)$$

In the region of the solubility product, there is a slight discrepancy between this data and other published data, but in the region of interest (bromide ion concentrations above 0.01) the agreement is good.

The temperature dependence of these stability constants is not known. However, the effect of temperature on the solubility product is known and is plotted in Figure 1. Drawing the best line through all the data gives an activation energy of 18,700 cal/mole. It should be mentioned that Klein (1956) gives a smaller temperature effect, with an activation energy of 10,200 cal/mole.

Assuming as a first approximation that the temperature dependency of all the stability constants is the same as for the solubility product, then

$$C_\infty = C_\infty^{18°} \times 10^{4080[(1/291.1)-(1/T°K)]} \quad (5)$$

These solubility relationships are plotted as Figure 2.

Differentiating Equation (5) with respect to C_{Br} gives

$$\frac{dC_\infty}{dC_{Br}} = 10^{4080[(1/291.1)-(1/T°K)]}[(-2.09 \times 10^{-13}/C^2_{Br} + 9.33 \times 10^{-6} + 2.10 \times 10^{-4}C_{Br} + 3.78 \times 10^{-4}C^2_{Br} + 8.36 \times 10^{-5}C^3_{Br}] \quad (6)$$

The bromide ion concentration in these regions of high free bromide (above 0.1 N) can be found by neglecting

any dissolved silver and assuming the free bromide is the initial bromide minus the amount of silver added, or

$$C_{Br} = \frac{C^0_{Br}V^0 - C^0_{Ag}Ft}{V} \tag{7}$$

Differentiating gives

$$\frac{dC_{Br}}{dt} = \frac{-FV^0(C^0_{Ag} + C^0_{Br})}{V^2} \tag{8}$$

The change in solubility with size is given by the well-known Gibbs-Thomson relationship (see, for example, Mullin, 1972)

$$C_r = C_\infty e^{K/r} = C_\infty \left[1 + (K/r) + \frac{(K/r)^2}{2!} + \ldots + \frac{(K/r)^n}{n!} + \ldots\right] \tag{9}$$

where

$$K = \frac{2\sigma V_m}{RT°K} = (0.00698\sigma/T°K)\mu m \tag{10}$$

Equation (10) is plotted in Figure 3 for $T = 60°C$ and $\sigma = 47.6$ dyne/cm. Figure 3 also gives the successive approximations to Equation (10). The first two terms, or

$$C_r/C_\infty \approx 1 + K/r \tag{11}$$

is an excellent approximation for all crystals with a radius

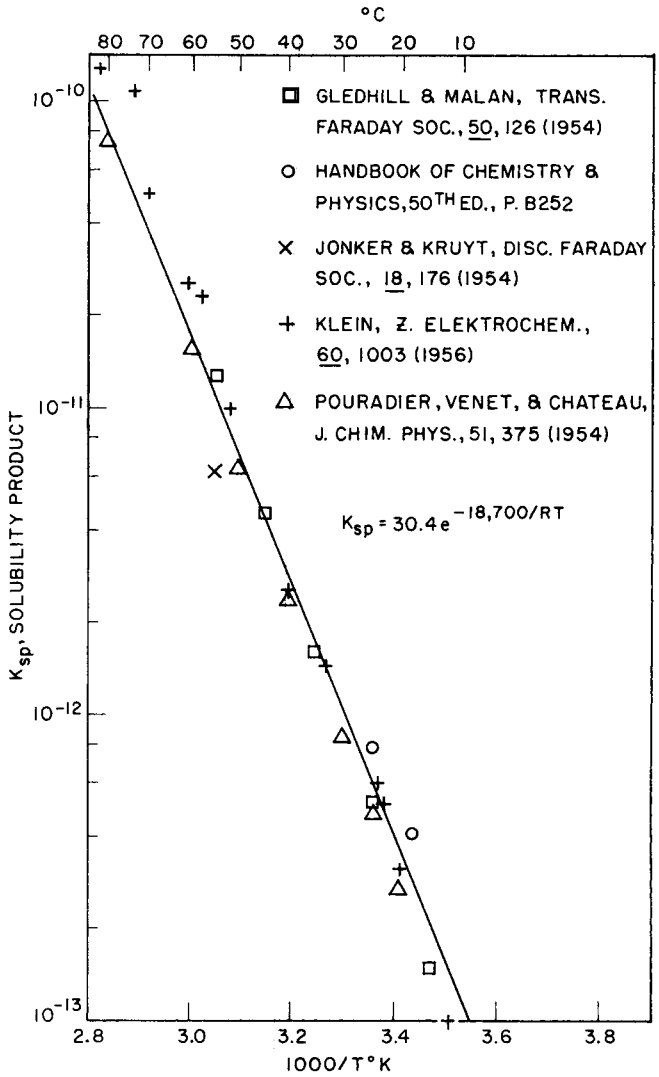

Fig. 1. Solubility product of silver bromide.

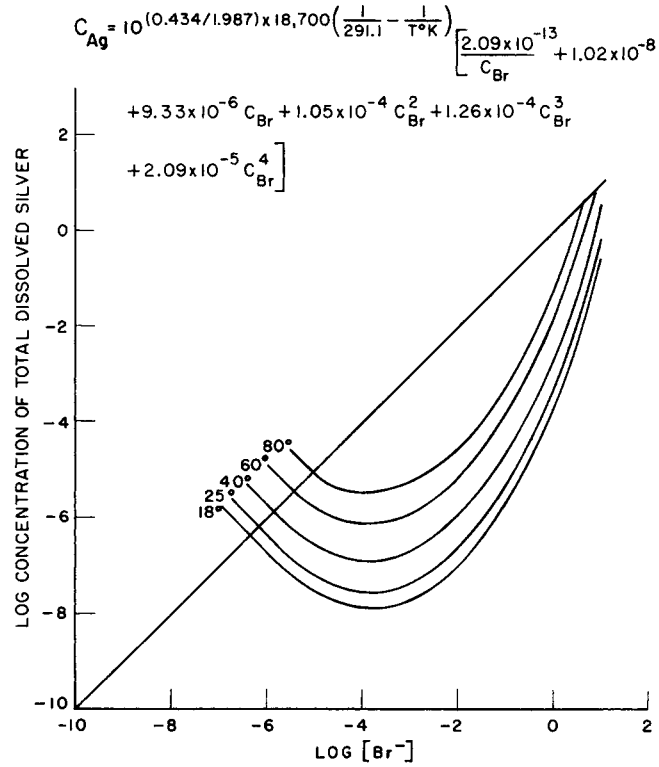

Fig. 2. Solubility of dissolved silver in excess bromide. The stability constants at 18°C are from Sillen (1963).

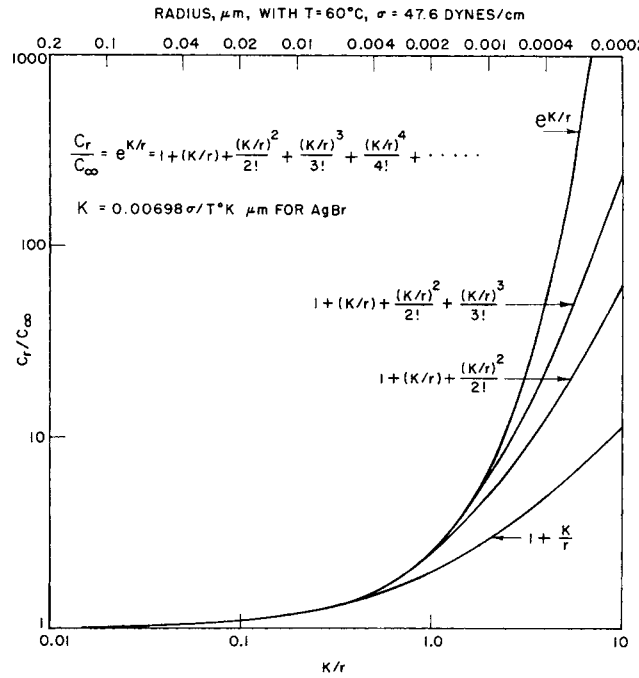

Fig. 3. Effect of crystal size on solubility.

over 0.004 μm, and we are assuming a nucleus size of about 0.05 μm. Even if the interfacial tension were as much as 10 times larger, or 476 dynes/cm, the approximation holds well for particles over 0.04 μm.

The actual interfacial tension of silver bromide is not known. Wagner (1961) used a value of 30 dynes/cm. Kahlweit (1961), quoted by Wagner (1961), suggests 20-40. Ljalikow (1955) suggests 120, Walton (1967) lists a calculated value of 161, and Nielson (1964) gives a value of 200. We will use a value of 30 dynes/cm and also a value of 300 to study the effects of surface

TABLE 1. SUMMARY OF RESULTS
The notation nEm means $n \times 10^m$

Run	Change from control	Nucleation times, s Start	Nucleation times, s End	No. crystals at end	Physical ripening, max. no. crystals No. at end	Physical ripening, max. no. crystals No. classes at end	$\bar{D}_n$, μm	Coef. var., %	Skewness	Highest EFF	Worst G-ERR
1	Control[a]	0.72	15.8	7.8E13	2.8	32	0.87	17	−1.06	1.09	0.05
2	$\sigma = 300$	7.08	10.2	3.1E12	21.9	61	2.53	20	−1.25	1.02	0.41
3	$T = 50°$	0.34	30.5	2.1E14	1.4	85	0.62	18	−1.34	1.04	0.03
4	$C^0_{Br} = 1.10$	0.48	22.1	1.4E14	1.9	54	0.71	20	−1.48	1.07	0.06
5	$b = 11$	0.72	13.2	6.9E13	1.9	68	0.91	18	−1.35	1.12	0.02
6	$k_2 = 10^{56}$	0.72	14.3	7.5E13	2.3	47	0.88	20	−1.44	1.11	0.01
7	$k_1 = 10^4$, $\Delta t = 1 \times 10^{-5}$	0.72	2.4	2.6E12	8.9	26	2.73	17	−0.91	1.04	0.09
8	$r_0 = 0.025\mu$m	1.43	5.9	8.4E13	6.5	141	0.85	19	−1.32	1.02	0.01
9	$\Delta t = 2.5 \times 10^{-5}$	0.72	15.9	8.1E13	2.8	28	0.85	22	−1.53	1.09	0.04
11	$t = 60$ min	1.44	16.8	2.8E13	4.3	23	1.23	17	−1.03	1.08	0.02
12	$b = 2$, $k_2 = 10^{26}$	0.72	31.3	1.1E14	5.7	4	0.78	21	−0.34	1.11	0.04
13	$b = 2$, $k_2 = 10^{24}$	0.72	18.0	8.0E13	3.3	25	0.86	19	−1.09	1.09	0.18
14	$\sigma = 300$, $\Delta t = 1 \times 10^{-5}$	7.07	10.1	2.7E12	25.2	5	2.73	9	−1.95	1.02	0.02
15	$\sigma = 300$, $k_1 = 10^2$	7.08	36.3	6.1E14	6.1	5	0.79	18	−0.41	1.01	0.01
16	$\sigma = 300$, $k_1 = 10^2$ $k_2 = 10^{56}$, $\Delta t = 3 \times 10^{-4}$	7.09	33.1	9.8E13	5.7	161	0.80	20	−1.28	1.01	0.01

[a] For the control $C^0_{Ag} = 0.60$, $C^0_{Br} = 1.30$, $C_{AgX} = 0.35$, precipitation time = 30 min., $T = 60°C$, $b = 10$, $\sigma = 30$ dynes/cm, $k_1 = 10^3$, $k_2 = 10^{58}$, $r_0 = 0.05\mu$m, and $\Delta t = 5 \times 10^{-5}$ min.

tension.

The growth equation now becomes

$$G_r = k_1 (C - C_r) \approx k_1 [C - C_\infty (1 + K/r)] \quad (12)$$

Substituting Equation (2) into Equation (12) gives

$$G_r = G_\infty - (k_1 C_\infty K/r) \quad (13)$$

Inserting Equation (13) into the growth term of Equation (1) and noting that the nth moment of the distribution curve μ_n is defined as

$$\mu_n \equiv \int_0^\infty f r^n dr \quad (14)$$

leads to

$$\int_0^\infty G_r f r^2 dr = G_\infty \mu_2 - k_1 C_\infty K \mu_1 \quad (15)$$

The nucleation rate may be taken as proportional to the bth power of the supersaturation, or

$$N = k_2 (C - C_{r0})^b \quad (16)$$

Substituting Equations (12) and (13) into (17) leads to

$$N = \frac{k_2}{{k_1}^b} \left(G_\infty - \frac{k_1 C_\infty K}{r_0} \right)^b \quad (17)$$

Equation (1) now becomes, after simplifying,

$$\frac{dG_\infty}{dt} = k_1 \frac{F}{V} (C^0_{Ag} - C_\infty) - \frac{F}{V} G_\infty + \frac{k_1 F V^0}{V^2} (C^0_{Ag} + C^0_{Br}) \frac{dC_\infty}{dC_{Br}} - \frac{4}{3} \pi {r_0}^3 \rho \frac{k_2}{{k_1}^{b-1}} \left(G_\infty - \frac{k_1 C_\infty K}{r_0} \right)^b - k_1 4\pi\rho G_\infty \mu_2 + {k_1}^2 C_\infty K \cdot 4\pi\rho \mu_1 \quad (18)$$

METHOD OF SOLUTION

The necessary equations were solved on an IBM 370 computer. The data read into the computer are the constants of the growth and nucleation equations, the size of the nucleus, the interfacial tension, the time interval of computation, and the description of the emulsion formulation. The constants of the growth and nucleation equation are chosen arbitrarily. It has been reported that homogeneous nucleation is the mechanism involved during the precipitation stage (Berry and Skillman, 1968). This is to be expected because of the highly insoluble nature of silver halides. We therefore took the exponent on the nucleation equation b as a high number, namely 10. However, if secondary nucleation were the mechanism involved, as is the case in most industrial crystallization processes, the exponent would be a small number. We also used $b = 2$.

The computation time interval is chosen to be small enough to give reasonable stability in the computations, and yet not extend the computation time unreasonably. Otherwise the computation time interval has little effect, as can be seen by comparing runs 1 and 9 in Table 1.

The computer solves Equation (18) for dG_∞/dt, and a new value of G_∞ is found by the Euler's method. During each time interval in the nucleation stage a new class of crystals is formed. From Equation (13) the new radius of the ith class is

$$r_i = r_{i,\text{old}} + [G_\infty - (k_1 C_\infty K/r)] \cdot \Delta t \quad (19)$$

The moments of the distribution are then evaluated and Equation (18) is solved again.

Details of the method of solution are given in Appendix A.*

The particle statistics—namely the average size, the standard deviation, the coefficient of variation, the skewness, and the kurtosis—are calculated from the moments of the distribution in the usual manner (Herdan, 1960). The definitions of these terms are given in Appendix A.

The equilibrium particle radius, which is the size for which the solution is just saturated and as such the crystals

* Appendices A and B have been deposited as Document No. 02375 with the National Auxiliary Publications Service (NAPS), c/o Microfiche Publications, 305 E. 46 St., New York, N.Y. 10017 and may be obtained for $1.50 for microfiche or $5.00 for photocopies.

neither grow nor dissolve, is found from the growth equation, Equation (13). The growth rate is set equal to zero, giving

$$r_{eq} = k_1 C_\infty K / G_\infty \qquad (20)$$

SUMMARY OF ASSUMPTIONS

It may be useful at this point to restate the assumptions made in the development of this model. They are

1. The precipitation vessel can be approximated as a well-mixed vessel.
2. The size of the effective nuclei are about the size of the smallest crystals normally visible in electron micrographs, about 0.1 μm in diameter.
3. The growth rate is directly proportional to the supersaturation; the dissolution rate for physical ripening (the negative growth rate) is directly proportional to the undersaturation, and both constants of proportionality are identical and equal to k_1.
4. McCabe's rule holds, and the growth rate is a function only of the supersaturation.
5. Solubility varies with size according to the Gibbs-Thomson relationship, which can be approximated by the first two terms of its series expansion. Supersaturation and growth rates will therefore also vary with size.
6. The nucleation rate is proportional to a power of the supersaturation measured with respect to the solubility of the nuclei.
7. All crystals are assumed spherical. In the discussion and in Appendix B* twinned crystals are considered.
8. The stability constants of the complex argentobromide species are assumed to vary with temperature in the same manner as the solubility product of silver bromide.
9. The growth and nucleation constants are chosen arbitrarily to give reasonable results and have no built-in temperature dependency.

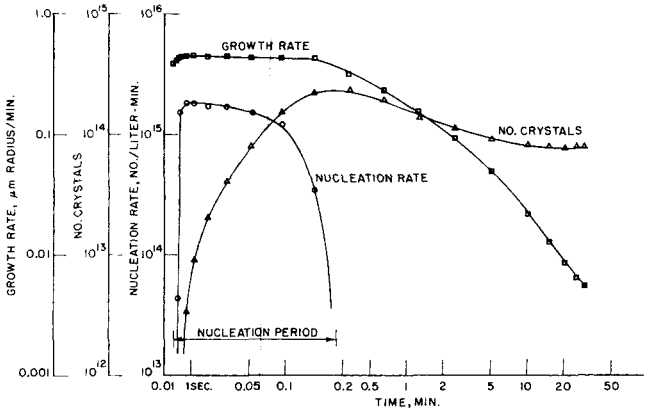

Fig. 4a. Computer simulation Run 1.

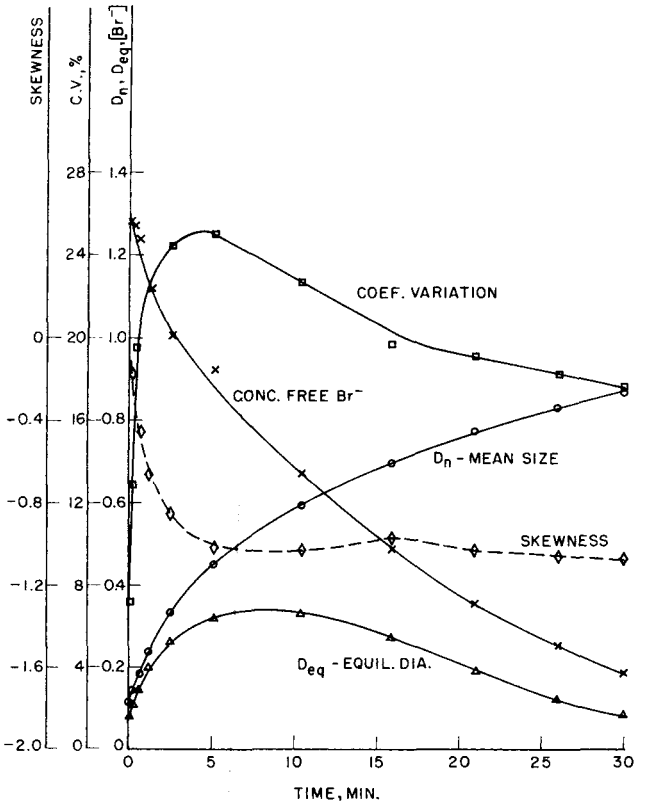

Fig. 4b. Computer simulation Run 1.

RESULTS

A summary of all the runs is given in Table 1. Figure 4 shows the changes in kinetic and crystal parameters during the course of the precipitation. The calculated decrease in the number of crystals with time is compared with the experimental data (Gutoff et al., 1974) in Figure 5.

DISCUSSION

Stability of Solution

The stability of the solution is tested by two internal checks. In one, the overall efficiency of utilization of silver, EFF, is calculated as the silver in the crystal divided by the silver added. It should start at zero when the initial silver stays in solution and gradually rise to unity. This efficiency may overshoot unity slightly and then drop back. The maximum values are given in Table 1.

The second internal check consists of calculating an instantaneous growth error, or the fractional difference in the amount of silver going into the crystals [as found from the growth and nucleation rates in Equation (18) multiplied by the system volume and the time interval] from the amount of silver in the increased volume of the crystals from the beginning to the end of the time interval. This value, called G-ERR, is usually zero. Its highest value is also shown in Table 1.

Effects of Growth and Nucleation Constants

The nucleation constants k_2 and b in Equation (16) have relatively little effect. Table 1 shows that increasing the exponent b from 10 to 11 (runs 1 and 5) gives only a slight, 4.6% increase in mean crystal size. The nucleation time is very slightly reduced. The physical ripening, as measured by the ratio of the maximum number of crystals to the number at the end is also slightly reduced.

The effect of k_2 is also small. Thus reducing k_2 from 10^{58} by two orders of magnitude (runs 1 and 6) increased the mean size by only 0.10 μm or 1%, and slightly reduced the nucleation time and the physical ripening. It did, however, noticeably increase the number of classes at the end. The same effects are seen when $b = 2$, by comparing run 12 with 13. Again, the lower k_2 gives a slightly larger crystal size, a smaller nucleation time, reduced physical ripening, and a significantly larger number of size classes at the end of the run. Increasing k_2 can lead to only one size class. We have arbitrarily chosen k_2 such that there are an adequate number of size classes. If k_2 is too low, then k_1, the growth constant, would have to be reduced to get the desired size. And the growth constant is al-

* See footnote on page 470.

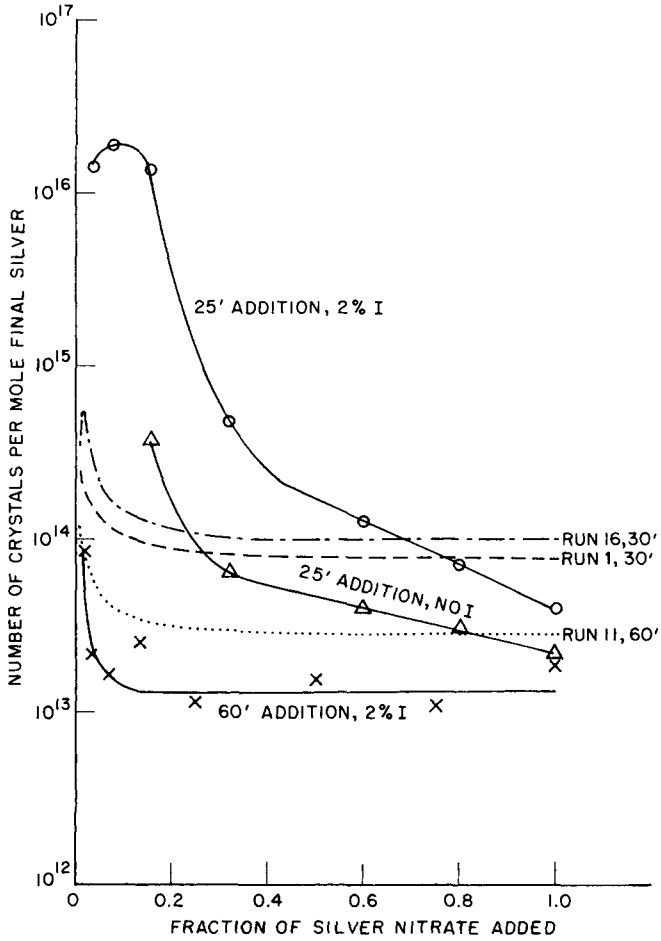

Fig. 5. Number of crystals present during precipitation. The experimental data are from Gutoff et al. (1974).

ready low compared to what would be expected from mass transfer calculations.

Based on mass transfer control the value of the growth constant k_1 is estimated to be about 10^6 $\mu m/min$ per mole/liter. However, Table 1 shows that to give reasonable crystal sizes of about 1 μm k_1 must be about 10^3. Increasing it as in run 7 to 10^4—still two orders of magnitude smaller than for mass transfer controlled growth—increases the mean size by a factor of 3 from 0.87 to 2.73 μm. Again, reducing k_1 by a factor of 10 (runs 16 and 14) lowers the mean size by a factor of 3.5.

The fact that the growth constant is so much smaller than for mass transfer controlled growth indicates that growth is controlled by kinetic considerations. This agrees with the conclusions of Hirata and Hohnishi (1966).

As the system is so sensitive to the growth constant and relatively insensitive to the nucleation constants, we may conclude that the system behavior is determined to a major extent by the growth kinetics. During the early stages, where nucleation occurs, the extent of nucleation is fixed by the growth rate. Material not incorporated into the growing crystals then goes to form nuclei or goes into increasing the supersaturation to satisfy the material balance.

EFFECT OF THE NUCLEUS SIZE

The radius of the nucleus was taken as 0.05 μm, as has been suggested by the smallest visible particles in electron micrographs (Gutoff et al., 1974). Run 8 with the nucleus assumed to be half this size gives just a 2% smaller average crystal size. However, it also gives a significantly smaller nucleation time, a greater degree of physical ripening, and a greater number of size classes at the end. We are uncertain about the correct value of the nucleus radius, but it does not seem to be too important as far as average size is concerned.

EFFECT OF THE INTERFACIAL TENSION

As mentioned earlier, suggested values of the interfacial tension of small silver bromide crystals range from 20 to 200. Increasing the value of the interfacial tension from 30 to 300 (runs 1 and 14) increases the resulting mean crystal size by a factor of 3. The degree of physical ripening was also greatly increased and the onset of nucleation was delayed. Even after reducing the growth constant by a factor of 10 to get the size down and reducing the nucleation constant k_2 by a factor of 100 to increase the number of size classes (run 16), there still is a high degree of physical ripening.

COURSE OF PRECIPITATION

Figure 4 shows, for run 1, the short period of nucleation and also the changes in time of the nucleation and growth rates and the crystal statistics. The growth rate gradually drops off once its maximum is reached. The average crystal size steadily increases. Part of the size increase is due to physical ripening shown by the decrease in the number of crystals once nucleation is over. The coefficient of variation, which is the standard deviation divided by the mean, in percent, goes through a maximum during the early stage of precipitation. The crystal size distribution starts off nearly symmetrical (zero skewness) and then the skewness levels off at a negative value. The equilibrium crystal size rises to a maximum and then decreases. Equation (20) shows that this size is proportional to the equilibrium solubility of the silver divided by the growth rate for large crystals. The solubility is given in Figure 2 as a function of the bromide ion concentration, which is shown in Figure 4 to decrease with time. Thus the solubility also decreases with time. The maximum in the equilibrium crystal size indicates that initially the growth rate decreases with time more rapidly than the solubility, while later on the solubility decreases more rapidly.

PHYSICAL RIPENING

Physical ripening causes the decrease in the number of crystals once effective nucleation is complete. In Figure 5 there are plots of experimental data along with data from the model showing the decrease in the number of crystals with time. In general, the predictions of the model are similar to the experimental data. However, the model shows an earlier start to physical ripening. In all cases the model predicts that the number of crystals levels off with time, while in two out of three experiments the number of crystals continues to decrease with time. Also, the predicted degree of physical ripening, as measured by the relative decrease in the maximum number of crystals, seems to be less than in the experimental data. From Table 1 it appears that the degree of physical ripening is greater for emulsions with larger mean size crystals. It also is greater for higher values of interfacial tension and smaller sizes of the nuclei. This may indicate that the effective nuclei size is smaller than 0.1 μm in diameter and that the interfacial tension of small silver bromide particles is in the upper end of the reported range of 20 to 200 dynes/cm. However, the 7-s delays in the onset of nucleation when the interfacial tension is 300 dynes/cm is excessively long.

The reason for the leveling off of the number of crystals with time in the model is not known. Perhaps the model would track better if the nucleus size were smaller and more terms were included in the series expansion of the Gibbs-Thomson solubility relationship. Perhaps the growth equation should have an exponent other than unity. Perhaps the model is just oversimplified.

EFFECT OF PRECIPITATION TIME

Table 1 shows that increasing the silver nitrate addition time from 30 to 60 min. (runs 1 and 11) increases the mean diameter by 46%. Trivelli and Smith (1940) reported that the mean area of bromide and iodobromide emulsion crystals are directly proportional to the precipitation time. The diameter of the average crystal would then be directly proportional to the square root of the precipitation time. For the doubling of time we have here the mean size should then increase by 41%, as $\sqrt{2} = 1.41$.

In one other published work (Gutoff et al., 1974), increasing the precipitation time from 25 to 60 min. increased the mean crystal size by 35%. A doubling of the time should then give an increased size of 30%. The increased size of 46% that the model predicts for a doubling of the precipitation time is reasonably close to the reported experimental values of 41% and 30%.

EFFECTS OF TEMPERATURE AND OF BROMIDE CONCENTRATION

Table 1 shows that lowering the temperature from 60° to 50°C (run 1 and 2) decreases the mean size by 29%. Also, decreasing the initial bromide concentration from 1.3 M to 1.1 M (run 1 and 4) decreases the mean diameter by 18%. These changes are in agreement with the literature where it has been reported that (Duffin, 1966; Zelikman and Levi, 1964) lowering the temperature or the bromide concentration significantly lowers the crystal size of silver halide emulsions. However, data on the magnitude of changes have not been published.

SKEWNESS AND COEFFICIENT OF VARIATION

Table 1 shows that the predicted coefficients of variation are almost all about 20%, and the skewness are all negative. Now it has been reported (Trivelli and Smith, 1940) that coefficient of variation on an area basis for a series of emulsions differing only in precipitation time is proportional to the average crystal area to the 0.03 to 0.19 power. The coefficient of variation on a diameter basis would then be almost independent of size. Almost all our coefficients of variation are the same, which agrees with this data. However, the actual coefficients of variation for pure bromide emulsions on an area basis are about 136% (Trivelli and Smith, 1940) which should be about half, or 68%, on a diameter basis. For iodobromide emulsion the coefficients of variation are 35 to 42%. Other data (Gutoff et al., 1974) give a coefficient of variation of 42% for a bromide emulsion and 42 and 52% for iodobromide emulsions. The model's predictions of 20% are too low.

Photographic emulsions tend to be positively skewed as is evident from published particle size distributions (Gutoff et al., 1974; Trivelli and Smith, 1940). The model here is deficient in that the skewnesses it predicts, while all small, are all negative.

TWINNED CRYSTALS

In normal silver bromide or iodobromide emulsions almost all the crystals are twinned—mostly plates—while the model assumes that all crystals are spherical. Multiple twinned crystals such as plates have two-dimensional growth rates up to 10 times greater than untwinned crystals (Gutoff, 1970, 1971). Also, this twinning and the higher two-dimensional growth rate appear to occur where the crystals reach a certain transition diameter (Gutoff, 1970, 1971) when the stacking faults are no longer able to diffuse out fast enough (Berry and Skillman, 1968). These features can be incorporated into the model, as is done in Appendix B, by assuming that crystals are all cubes until they reach a certain transition diameter, when a larger two dimensional growth occurs to form square prisms. With no increase in two-dimensional growth so that all the crystals are cubes at all times the coefficient of variation is about 45%. With larger two-dimensional growths the coefficient of variation can be over 100%. However, the skewness is still negative.

NOTATION

b = exponent in the nucleation equation [Equation (16)], dimensionless
C = concentration of dissolved silver, mole/liter
C^0_{Ag} = concentration of silver nitrate, mole/liter
C^0_{Br} = initial concentration of bromide, mole/liter
C_{Br} = concentration of free bromide, mole/liter
C_{AgX} = final concentration of silver halide, mole/liter
C_r = concentration of dissolved silver in equilibrium with crystals of radius r, mole/liter
C_∞ = concentration of dissolved silver in equilibrium with large crystals, mole/liter
$\overline{D_n}$ = number mean crystal diameter, μm
F = flow rate of silver nitrate, liter/min
f = frequency function. fdr is the number of crystals per liter with a radius between r and $r + dr$, number/liter-μm
G_r = radial growth rate for crystals of radius r, μm/min
G_∞ = radial growth rate for large crystals, μm/min
k_1 = proportionality constant in the growth equation [Equation (2)], μm/min per mole/liter
k_2 = proportionality constant in the nucleation equation, Equation (16)
K = constant in the Gibbs-Thomson relationship [Equation (9)], μm
M = number of moles in a crystal
n = exponent in Equation (14), dimensionless
R = gas constant, in consistant units for Equation (10), 8.314×10^3 dynes-cm^2/mole-°K-μm
r = crystal radius, μm
r_{eq} = radius of crystals in equilibrium with the solution
r_i = radius of crystals in the ith size class, μm
r_0 = nuclei radius, μm
T = temperature, °C or °K
t = time, min
V = volume, liter
V^0 = initial volume of the halide solution, liter
V_m = molar volume of silver bromide, 29.0 cm^3/mole

Greek Letters

ρ = molar density of silver bromide, mole/μm^3
σ = interfacial tension of silver bromide crystals, dynes/cm
μ_n = nth moment of the size distribution, defined by Equation (14), μm^n/liter

LITERATURE CITED

Berry, C. R., and D. C. Skillman, "Fundamental Mechanisms in Silver Halide Precipitation," *J. Phot. Sci.*, **16**, 137 (1968).
Duffin, G. F., *Photographic Emulsion Chemistry*, pp. 57-58, 63, Focal Press, London (1966).

Gutoff, E. B., "Nucleation and Crystal Growth Rates During the Precipitation of Silver Halide Photographic Emulsions," *Phot. Sci. Eng.*, **14**, 248 (1970).
———., "Nucleation and Crystal Growth Rates During the Precipitation of Silver Halide Photographic Emulsions. II. Ammoniacal Emulsions," *ibid.*, **15**, 189 (1971).
———., F. R. Cottrell, G. Margolis, E. G. Denk, and C. H. Wallace, "Crystallization Mechanisms During the Precipitation of Silver Halide Photographic Emulsions," *ibid.*, **18**, 8 (1974).
Herdan, G., *Small Particle Statistics*, 2nd edit., Butterworths, London (1960).
Hirata, A., and S. Hohnishi, "Growth Mechanism of Monodisperse Silver Bromide Particles in Gelatin Solution," *Bull. Soc. Sci. Phot. Japan*, **16**, 1 (Dec., 1966).
Kahlweit, M., "Kinetics of Phase Formation in Condensed Systems. III. Critical Oversaturation of Aqueous Electrolyte Solutions," *Z. Physik. Chem.* (Frankfurt), **28**, 245 (1961).
Klein, E., "Solubility of Silver Halide in Sulfite Solutions," *Z. Elektrochem.*, **60**, 1003 (1956).
Ljalikow, K. S., "Theory of Physical Ripening of Photographic Emulsions," *Z. Wiss. Phot. Photophysik Photochem.*, **50**, 151 (1955).
Mullin, J. W., *Crystallization*, 2nd edit., pp. 222, Butterworths, London (1972).
Nielson, A. E., *Kinetics of Precipitation*, pp. 64, Pergammon, Oxford, London (1964).
Randolph, A. D., and M. A. Larson, *Theory of Particulate Processes*, Academic Press, New York (1971).
Sillén, L. G., "Stability Constants of Metal Ion Complexes," 2nd. edit., Sect. I, pp. 323-24, The Chemical Soc., Special Pub. #17, London (1964); data of V. E. Mironov, "A Radiochemical Study of the Solubility of Silver Halides and Their Analogy with the Halides of Univalent Thallium," *Radiokhimiya*, **5**, 118 (1963).
Trivelli, A. P. H., and W. F. Smith, "Effect of Silver Iodide upon the Structure of Silver Bromo-Iodide Precipitation Series," *Phot. J.*, **80**, 285 (1950).
Wagner, C., "Theory of the Aging of Precipitates by Recrystallization (Ostwald-Ripening)," *Z. Elektrochem.*, **65**, 581 (1961).
Walton, A. G., *The Formation and Properties of Precipitates*, pp. 123, Interscience, New York (1967).
Zelikman, V. L., and S. M. Levi, *Making and Coating Photographic Emulsions*, (transl. of Russian edit.), pp. 75,79, Focal Press, London (1964).

Manuscript received November 6, 1973; revision received February 15 and accepted February 22, 1974.

An Experimental Investigation of Viscous Heating in Some Simple Shear Flows

Theoretical investigations of viscous heating in the flow of fluids with an exponential dependence of viscosity on temperature have shown that, for a given shear stress, two shear rates are possible. Above a critical value, the stress decreases as the shear rate increases.

The present work is an experimental study of this phenomenon in plane and circular Couette flows and in cylindrical Poiseuille flow. Arochlor^{R} 1260, a high viscosity Newtonian fluid with an extremely sensitive viscosity-temperature dependence is used as the test fluid. The results clearly show that two shear rates for Couette flow exist for one measured wall shear stress. Because of the viscosity-pressure dependence of the fluid, the Poiseuille flow results are inconclusive.

PETER C. SUKANEK
and
ROBERT L. LAURENCE

Department of Chemical Engineering
University of Massachusetts
Amherst, Massachusetts 01002

SCOPE

Rheologists have long been aware of the impossibility of maintaining viscous flow without some dissipation of mechanical energy into heat. For the past 50 years, investigators in many fields have attempted to estimate and measure the magnitude of the temperature rise due to frictional heating and the effect this increased temperature has on measured flow properties.

One of the most significant results of previous investigations is the existence of a maximum shear stress, below which, for a given stress, the shear rate assumes two values. At low fluid speeds, the stress increases because of the increased shear rate. As the speed increases, the vis-

Correspondence concerning this paper should be addressed to R. L. Laurence. P. C. Sukanek is with the USAF Rocket Propulsion Laboratory, DYSP, Edwards AFB, California 93523.